24 Patient-Specific Instrumentation and 3-D Osteotomy

Wouter Van Genechten, Annemieke van Haver, and Peter Verdonk

24.1 Introduction

Osteotomies around the knee are well-established, joint-preserving surgical interventions which primarily aim to correct the mal-aligned lower limb in the coronal plane, hereby inducing mechanical unloading of either the medial or lateral arthritic knee compartment [1]. In neutral alignment, the medial compartment bears up to 55–70% of a person's weight during the stance phase of gait, which increases with 5% for every 1° of additional varus deformity [2]. The fact that a constitutional varus alignment of 3° or more is found in a significant number of adults, contributes to the overall high prevalence of medial relative to lateral knee osteoarthritis (OA) [3–5]. Consequently, osteotomies towards valgus are most commonly performed, and since varus deformities are frequently found in the proximal tibia (mechanical medial proximal tibial angle (mMPTA) < 85°), surgical corrections are preferred at this level. Both the medial opening-wedge and the lateral closing-wedge high tibial osteotomy (HTO) have shown to be effective for unloading the diseased medial compartment [6]. When performed in a timely fashion, it can delay or even prevent the development to end-stage knee OA [7]. For several reasons such as the need for a fibular osteotomy, risk of peroneal nerve damage, and extended soft tissue dissections, the lateral closing-wedge approach has fallen into disuse [2, 6, 8]. Therefore, modern opening-wedge HTO forms currently the standard with reported survival rates of >90% at 10 years in young (<65 years) and physically active patients [8–10]. Nevertheless, conventional opening-wedge HTO remains a technically demanding procedure with a considerable risk of complications, including (unstable) lateral hinge fractures, delayed or non-union of the gap, over/under-correction, and unintended increase of the tibial slope [11–14].

Considering the accuracy of conventional HTO procedures in the coronal plane, Van den Bempt et al. uncovered a surprisingly low achievement of the planned correction [15]. Eight out of 11 conventional HTO cohorts were unable to reach a threshold of 75% accurate corrections

W. Van Genechten (✉)
More Institute, Antwerp, Belgium

University of Antwerp, Antwerp, Belgium

A. van Haver
More Institute, Antwerp, Belgium

P. Verdonk
More Institute, Antwerp, Belgium

University of Antwerp, Antwerp, Belgium

ORTHOCA, Antwerp, Belgium

© ISAKOS 2022

N. Nakamura et al. (eds.), *Advances in Knee Ligament and Knee Preservation Surgery*,
https://doi.org/10.1007/978-3-030-84748-7_24

within a self-defined accuracy interval. Since realignment surgery is a highly individualized intervention associated with a small tolerance for error, these results are posing a major concern regarding intervention durability [16]. Both unprecise preoperative osteotomy planning and subsequent challenging translation into surgery are considered to form the basis of inaccurate osteotomy corrections [17]. The introduction of computer navigation in the field of knee osteotomies has certainly been a step towards more accurate surgical outcomes, mainly due to the real-time visualization of the corrected limb [18]. However, expensive equipment, a long learning-curve with prolonged surgical duration and unpredicted technology failure have constrained this approach from becoming widespread among orthopaedic knee surgeons [15, 19].

Since modern volumetric imaging modalities such as very low-dose computer tomography (CT) scans and magnetic resonance imaging (MRI) became available on large-scale, several attempts have been made to virtually simulate surgeries in suitable medical software and to print 3-D anatomical models [20]. Shortly afterwards, the intra-operative use of 3-D-printed patient-specific instrumentation (PSI) was introduced, first in maxillofacial surgery which was later successfully translated to surgical corrections of the spine and mal-union fractures of the forearm [21–23]. The implementation of PSI in realignment surgery of the lower limb, however, is relatively new [24]. The thought of having customized surgical tools available during surgery, which instantly determine the osteotomy plane together with the intended correction in both the coronal and sagittal plane, sounded very appealing and led to the development of a handful innovative PSI approaches for knee osteotomies [16, 25–28]. Therefore, this chapter provides an overview about the clinical use of 3-D osteotomy planning, customized guide printing and PSI in the operating room (OR) with accuracy outcomes of several techniques developed for knee osteotomy surgery. Further, the author's onsite preferred PSI approach is discussed, together with general considerations and concerns about the topic.

24.2 Osteotomy Planning

A proper full-leg bipodal standing radiograph has always been the benchmark both for determining mal-alignment of the lower limb and for osteotomy planning [29]. However, questions have been raised about the reliability and effect of slight knee flexion and limb rotation on 2-D image measurements [30–32]. Moreover, the factor weight-bearing might cause an overestimation of the preoperative varus alignment, which should theoretically result in high numbers of overcorrected osteotomies [33–35]. Finally, full-leg radiographs only allow osteotomy planning in a single plane (coronal), while most HTO surgeries consist of a biplanar bone cut.

Despite the imperfections, a full-leg standing radiograph still forms a cornerstone in the planning phase, even in the majority clinical PSI studies (Table 24.1) [14, 25–27, 36, 37]. Now, considering 3-D bone modelling for osteotomy planning, a baseline CT-scan appears to be the better option over MRI because it is less expensive, the imaging waiting times are shorter, and it provides clearer spatial resolution to segment the bones [38]. A scan of the knee joint, or at minimum of the proximal tibia is obligatory to perform a multiplanar osteotomy simulation and to design PSI. The obtained imaging DICOM files from the scan are easily loaded into the dedicated segmentation software after which the anatomical bone models are exported as STL-files to maintain scale and composition. Finally, the bone models are transferred to 3-D medical planning software to virtually pre-plan the correction size and define the bone cut (plane, depth and starting point) which is ultimately followed by PSI design and printing. [25, 26, 36, 37].

Some authors have recently implemented the mechanical medial proximal tibial angle (mMPTA) as primary planning angle. [25, 37] The mMPTA strictly limits the correction change to the tibial bone in contrast to the mechanical femorotibial angle (mFTA) or weight-bearing line (WBL%) which might be prone to variation by a patient's position during preoperative imaging. Moreover, this angle has proven to be the only predictor for alignment errors after opening-

Table 24.1 Overview of laboratory and clinical studies using patient-specific instrumentation (PSI) for osteotomy surgery around the knee joint

Author (Year)	# PSI cases (HTO/DFO)	Planning	Target (planning)	PSI Technique	Accuracy with PSI		Conventional controls	Postop measurements (2D/3D)
					Coronal plane	Sagittal plane		
Laboratory studies								
Kwun et al. (2017)	10 Porcine HTO	2-D and 3-D simulation	62.5%	Printing of gap volume (wedge)	Postop: 61.8% ± 1.5	Pre: 11.2° ± 2.2 Post: 11.4° ± 2.5	No	2-D
Donnez et al. (2018)	10 Human HTO	3-D simulation	Random	Cutting guide with pre-drilled matching holes for final plate	ΔmMPTA: 0.2° ± 0.3 (−0.3° to 0.5°)	ΔTS: −0.1° ± 0.5 (−0.7° to 0.8°)	No	3-D
Clinical studies								
Victor et al. (2013)	4 HTO/10 DFO	3-D simulation	Variable	Cutting guide with pre-drilled matching holes for final plate	ΔmFTA: 0° ± 0.72 (−1° to 1°)	ΔTS: 0.3° ± 1.14 (−0.9° to 3°)	No	2-D
Perez-Mananez et al. (2016)	8 HTO	2-D planning and 3-D simulation knee	62%	Cutting guide with 3 spacer wedges	ΔmFTA: 0.5° (0° to 1.2°)	Not mentioned	Yes ($n = 20$)	2-D
Arnal-burro et al. (2017)	12 DFO	2-D planning and 3-D simulation knee	62%	Cutting guide with 3 spacer wedges	ΔmFTA: 0.28° (0° to 1°)	Not mentioned	Yes ($n = 20$)	2-D
Munier et al. (2017)	10 HTO	Full leg 2-D and full-leg 3-D simulation	HKA: 2-4° valgus	Cutting guide with pre-drilled matching holes for final plate	100% within [−2°;+2°] mFTA	90% within [−2°;+2°]	No	2-D and 3-D
Yang et al. (2018)	10 HTO	2-D planning and 3-D simulation knee	62.5%	Biplanar cutting guide with holes for rod matching	Postop: 60.2% ± 2.8%	Preop: 9.9° ± 0.47 Postop: 10.1° ± 0.36	No	2-D
Kim et al. (2018)	20 HTO	2-D planning and 3-D simulation knee	62.5%	Printing of gap volume (wedge),	ΔWBL: 3.9% ± 4.5	Preop: 9.6° ± 3.3 Postop: 9.8° ± 3.2	No	2-D

(continued)

Table 24.1 (continued)

Author (Year)	# PSI cases (HTO/DFO)	Planning	Target (planning)	PSI Technique	Accuracy with PSI		Conventional controls	Postop measurements (2D/3D)
					Coronal plane	Sagittal plane		
Kim et al. (2018)	20 HTO	2-D planning and 3-D simulation knee	62.5%	Printing of gap volume (wedge), no slot for bone cut	ΔWBL: 2.3% ± 2.5	Preop: 8.6° ± 3.3 Postop: 8.9° ± 3.1	Yes (n = 20)	2-D
Jones et al. (2018)	18 HTO	3-D simulation	Not mentioned	Cutting guide position based on distant landmarks and 'correction block'	100% within [-3°;+3°] mFTA	100% within [-3°;+3°] TS	No	3-D
Chaouche et al. (2019)	100 HTO	Full leg 2-D and full-leg 3-D simulation	Not mentioned	Cutting guide with pre-drilled matching holes for final plate	ΔmFTA: 1.0° ± 0.9 ΔmMPTA: 0.5° ± 0.6	ΔTS: 0.4° ± 0.8	No	3-D
Fucentese et al. (2020)	23 HTO	Full leg 2-D and full-leg 3-D simulation	Majority on 62.5%	Cutting guide with pre-drilled matching holes for final plate	ΔmFTA: 0.8° ± 1.5 74% within [−2°;+2°] mFTA	ΔTS: 1.7° ± 2.2 61% within [−2°;+2°] TS	No	2-D and 3-D
Authors (2020)	10 HTO	3-D simulation (full-leg)	Lateral spine	Customized wedge and cast for structural bone graft	ΔmFTA: -0.4° ± 1.0 100% within [−2°;+2°] mFTA	ΔTS: 2.1° ± 2.6	No	2−D and 3-D

HTO high tibial osteotomy, *DFO* distal femur osteotomy, *Δ* difference, *mMPTA* mechanical medial proximal tibial angle, *mFTA* mechanical femorotibial angle, *WBL* weight-bearing line, *TS* tibial slope

wedge HTO and makes its inclusion in modern HTO planning recommendable to improve correction accuracy [39]. In addition, the authors support the conduction of mMPTA measurements in order to control joint line orientation ((JLO) <5°) after HTO and to maintain the conversion option to arthroplasty in a later stadium. The planned mMPTA should not exceed 95° as this might induce excessive joint line obliquity with increased shear stress on the articular cartilage [40]. A double-level osteotomy might be indicated in large varus corrections which can, on their turn, be planned more precisely in 3-D imaging software. In one PSI strategy, final plate type and positioning are already included in the 3-D planning by determining the predrilled screw holes in the PSI guide (Fig. 24.1). [14, 24, 25, 37] This eventually facilitates immediate and correct implant positioning intraoperatively but leaves a small margin for unexpected alternations during surgery.

Chernchujit et al. recently reported on a planning technique to correct the non-weight bearing component of a full-leg supine CT-scan by using a 2-D full-leg standing radiograph [41]. Accordingly, a full-leg 3-D model under 'weight-bearing circumstances' was created to simulate the intended osteotomy; however, no PSI was printed or used intraoperatively. Despite precise 3-D planning, only 79% of cases ($n = 19$) fell into a wide ±3° range around target, which emphasizes the actual need for customized surgical tools during surgery on top of preoperative 3-D simulation [41].

Overall, the main advantages of executing a preoperative 3-D osteotomy planning are (1) the reliable angle measurements based on exact identification of unique bony landmarks, (2) the multiplanar and multilevel simulation of the surgery and finally (3) the ideal tool for designing PSI and tailor-made anatomical models [42]. With the availability of 3-D bone models, the intended correction size can be planned very precisely in a way that even the thickness of the sawblade can be taken into account [16].

24.3 3-D Printing of PSI: Materials and Equipment

The availability of 3-D planning software, medical grade resin, a 3-D printer and most importantly, trained personnel are mandatory for streamlining an in-hospital preoperative planning and printing process of PSI. If one of these requirements onsite is missing, external companies can be involved; however, this may result in an increased cost per case, a longer manufacturing process and more complex logistics. Therefore, it can be recommended for certain hospitals/orthopaedic departments to invest in a 3-D core facility, especially in case of high surgical turnovers and short waiting lists. Moreover, 3-D planning and PSI is far from only reserved

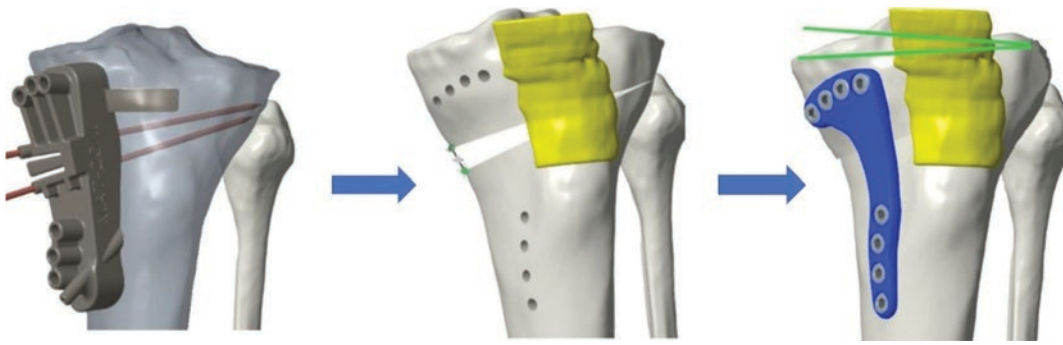

Fig. 24.1 Design of a customized osteotomy guide equipped with drill holes which eventually match with the screw holes of the plate during optimal (planned) gap distraction in opening-wedge HTO. Final plate type and positioning are included in the 3-D osteotomy planning. (Donnez et al. [45], Munier et al. [25], Chaouche et al. [37]; permission from the authors was obtained to publish illustrations)

for knee osteotomies. PSI has proven its value in multiple disciplines and operations such as maxillofacial/craniofacial surgery, bone tumour resections, osteotomies for mal- or non-union fractures and corrections of forearm deformities [43]. So theoretically, a 3-D core facility can supply several departments of interest, hereby sharing the costs of its own establishment and maintenance.

When used in the OR, anatomical patient models and PSI are printed in medical grade resin. Polyamide (or nylon) is the most commonly used material for guide manufacturing because of its biocompatibility and good mechanical properties [14, 16]. When devices are printed with selected laser sintering (SLS), the polyamide powder is fused into a solid model, which does not need structural support. Further, acrylonitrile butadiene styrene (ABS), a thermoplastic polymer, forms another choice and has been frequently used to print PSI guides for knee osteotomies [26, 27, 44]. Using this material, Perez-mananez was able to print PSI for less than €5 euro per patient, based on an ABS purchase price of €0.04/gram [26]. Arnal-burro et al. used polylactic acid (PLA), a thermoplastic polyester, and was able to print the required PSI per patient for even half of this price [36]. His group proposed a reasonable price range of €500–2000 for purchasing a suitable 3-D printer compatible with this material. The drawback of these inexpensive fused deposition modelling (FDM) 3-D printers, however, is the lower printing accuracy and the obvious layer lines which are inherent to filament printing. Since 2016, it is also possible to 3-D print medical grade photopolymer resins with a desktop stereolithography (SLA) printer, which offers a high resolution, accuracy and a smooth surface finish. A drawback of SLA printing is that the models need support structures which require manual removal after printing. Nevertheless, the authors have been using this printing technique for several years onsite with overall satisfying outcomes. Finally, the device should be safely sterilized in a standardized steam pressure autoclave, gamma ray sterilization or low temperature hydrogen peroxide sterilization (STERRAD sterilization) according to the instructions on the technical data sheet of the used material [14, 16, 28].

24.4 PSI Techniques and Accuracy

In a recent controlled laboratory study, the importance of PSI cutting guides was highlighted for improving osteotomy accuracy [17]. Customized slot guides (closed) were compared to open guides and free-hand sawing on a mid-shaft femur model. The closed guides had favorable outcomes in both precision of the osteotomy cut and translation of the preoperative 3-D planning. The authors concluded that the use of PSI guides (open and closed) leads to more predictable outcomes in osteotomy surgery and bony resections and can be recommended especially in multiplanar and rotational corrections [17].

In the context of osteotomies around the knee joint, PSI guides can be beneficial in two ways: first by defining the starting point, inclination angle and plane for the actual bone cut(s) and secondly by determining the planned gap opening at the medial cortex. Victor et al. designed and clinically tested the first PSI prototype for knee osteotomies (HTO and distal femur osteotomies (DFO)) which included a robust frame for fitting patient's bony landmarks to assure proper positioning (Table 24.1) [24]. This guide was equipped with a cutting slot and drill holes which would later match with the screw holes of the fixation plate as under optimal gap distraction (Fig. 24.2). After 14 cases, an accuracy outcome of 0° ± 0.72 ΔmFTA relative to the planning was found in the coronal plane with all cases falling within [−1°; +1°] around the target. Overall, minor changes were observed in the sagittal plane. Despite these highly accurate results, a large incision (13 cm femur and 12 cm tibia) and soft tissue dissection was required to properly fit the guide, inducing higher risk for wound infections and delayed or non-union of the gap [16]. Nevertheless, this pioneer technique was later adopted by several research groups developing their own PSI technique for opening-wedge

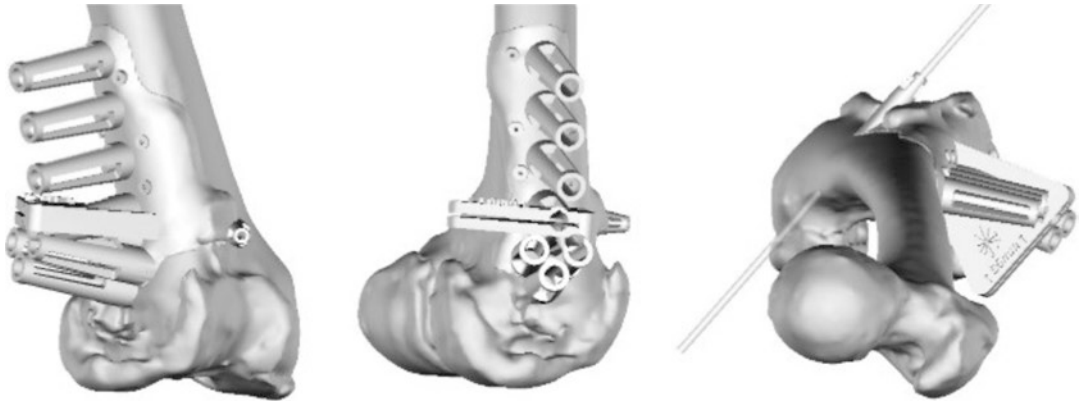

Fig. 24.2 Design of the first PSI guide for osteotomies around the knee (distal femur osteotomy (DFO)). (From Victor et al. [24]; permission from the corresponding author was obtained for illustration reprinting)

Fig. 24.3 Intraoperative positioning and fixation of a PSI cutting guide in opening-wedge HTO. (Donnez et al. [45], Munier et al. [25], Chaouche et al. [37]; permission from the authors was obtained to publish illustrations)

HTO. [14, 25, 37, 45] The largest case series with PSI was recently published by Chaouche et al., who included 100 opening-wedge HTO cases (Figs. 24.1 and 24.3) [37]. In the coronal plane, an accuracy of 1.0° ± 0.9 ΔmFTA and 0.5° ± 0.6 ΔmMPTA was established, while the planned and postoperative tibial slope differed with 0.4° ± 0.8. The authors concluded that by applying this PSI technique, predictable correction outcomes can be delivered, without increasing (non-)specific HTO complications [37].

To avoid large skin incisions for robust PSI guides, Jones et al. developed an external device to align the osteotomy cutting guide based on distant superficial bony landmarks including the fibular head and maleolli [16]. His group suggested to use a customized 'correction block' fixed with 3 k-wires to determine and maintain the intended gap opening during surgery. Preliminary results with this technique ensure an accuracy within 3° around the target after 18 HTO cases [16]. In this way, an HTO can be performed minimally invasive while maintaining freedom for the surgeon to choose the fixation device and plate positioning. However, the authors admit to a longer multi-step procedure which is in conflict with a principal advantage of PSI, namely, reducing the time and complexity of the operation [17, 26, 36].

Another way to obtain the planned limb realignment is simply to print the complementary wedge spacers needed to fill the osteotomy gap [26, 27, 44]. Perez-Mananez et al. described this approach by exchanging the spacers for structural bone autograft derived from the iliac crest in 8 HTO cases [26]. In combination with a custom-

ized positioning guide, an average accuracy of 0.5° ΔmFTA (ranging 0°–1.2°) was demonstrated. Twenty conventional control HTOs were performed, and although showing lower accuracy (average 1.1° ΔmFTA (ranging 0°–2.8°)), both groups were not significantly different. Interestingly, an additional 3-D anatomical model of the proximal tibia was always available intraoperatively to confirm fitting of the cutting guide. Shortly thereafter, the exact same PSI approach was evaluated for 12 DFOs and compared to the conventional technique [36]. Mechanical axis deviation in the coronal plane was on average 0.28° ΔmFTA (ranging 0°–1°) for PSI and 1.8° ΔmFTA (ranging 0°–4°) in controls, which was significantly different.

Similarly, but without the inclusion of an osteotomy cutting guide and the implementation of bone autograft, Kim et al. demonstrated a lower absolute difference from the correction target of 62.5% in 20 PSI HTO cases (2.3% ± 2.5 ΔWBL) compared to 20 conventional controls (6.2% ± 5.1 ΔWBL) [27]. The tibial slope remained almost unchanged in the PSI cases, while for the conventional approach, a statistically significant increase was observed. Finally, Yang et al. found an alternative way to obtain the desired wedge opening by designing a biplanar cutting guide consisting of a proximal and distal part, each equipped with an aligning hole [28]. While distracting the osteotomy, a metal rod was placed in the proximal hole and only fitted in the second distal hole of the guide when the planned osteotomy gap was obtained. A pilot study of 10 HTOs yielded a postoperative alignment of 60.2% ± 2.8 while aiming for 62.5% and a tibial slope that barely increased relative to the preoperative status.

24.5 PSI Technique of the Authors

24.5.1 3-D Planning

Preoperatively, the patient receives a full-leg bipodal standing radiograph and a supine CT-scan of the affected limb according to the Trumatch knee scanning protocol [38]. This low-dose protocol is specially designed for creating 3-D models by scanning the anatomical reference points, including hip and ankle joint at 5 mm slice thickness and spacing and the knee joint at 0.5 mm slice thickness and spacing in a 150 mm range. The resultant Digital Imaging and Communications in Medicine (DICOM) files are loaded into the segmentation software Mimics® (Materialise®, Heverlee, Belgium) to separate bony structures from surrounding soft tissue. The 3-D model of the lower limb is then transferred to the planning software 3-matic® (Materialise®, Heverlee, Belgium), in which the desired osteotomy cut and wedge opening are simulated, aiming for the postoperative mechanical axis to pass through the lateral spine (Fig. 24.4). All osteotomies are simulated using the mMPTA as main planning angle. At the end of the planning process, a personalized fitting wedge and cast are designed and 3-D printed in certified biocompatible photopolymers and sterilized by hydrogen peroxide gas plasma (Fig. 24.5). For safety reasons, the printed cast is labeled with the surgery side, the amount of correction (°) and the patient's initials. To ensure proper positioning of the printed wedge in the osteotomy gap, two grooves are created which should match with the medial cortex of the proximal and distal tibial fragment. Although this planning method looks seemingly time-consum-

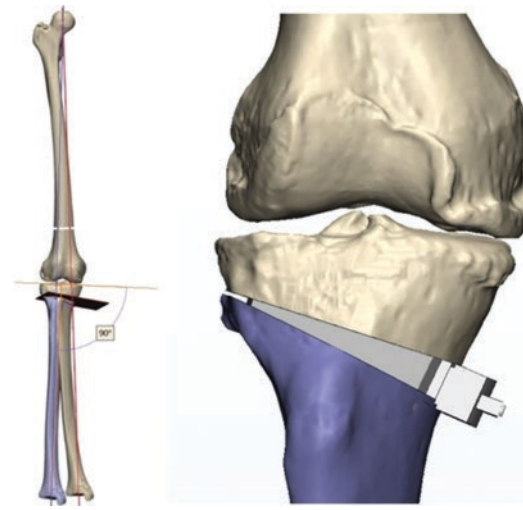

Fig. 24.4 Alignment determination on a 3-D bone model of the lower limb with virtual 3-D HTO planning and required gap opening/spacer size

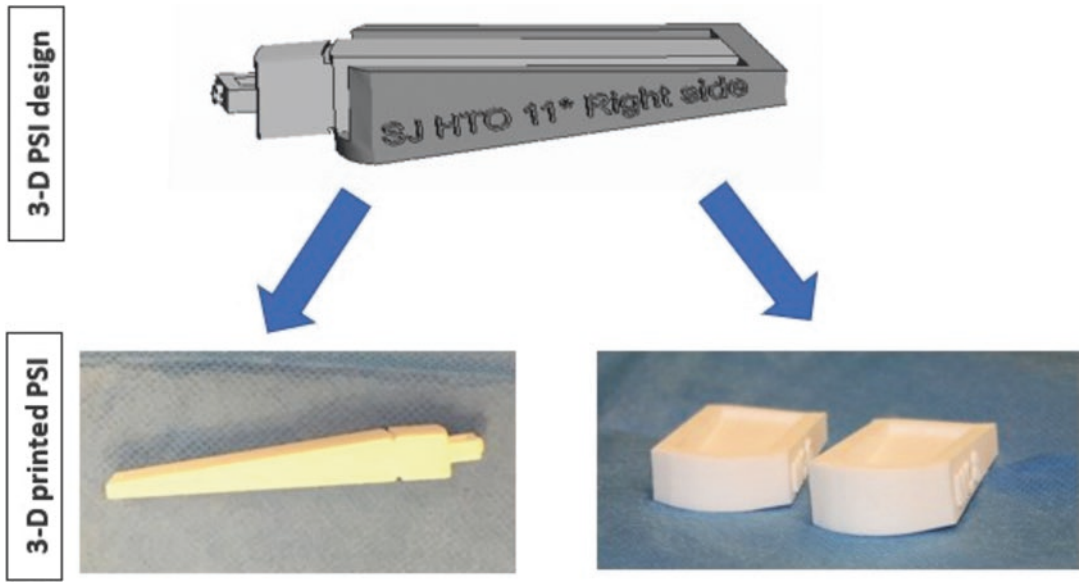

Fig. 24.5 Final design and 3-D printed models of the wedge spacer with complementary cast to trim customized bone allograft

ing, the time from scanning the lower extremity up to the availability of sterilized PSI in the OR can be fit in a 48 h streamlined flow due to the onsite availability of the required software, resin and 3-D printing equipment.

24.5.2 Surgical Technique for MOW-HTO

A vertical medial skin incision is made on the tibia. Under fluoroscopic control, two parallel K-wires are introduced horizontally, starting 3–4 cm below the medial tibial joint line on the medial cortex and aimed laterally, proximally of the tibiofibular joint and 1 cm below to the lateral joint line. The horizontal osteotomy is performed distal in contact with the 2 K-wires on the medial side using an oscillating saw, followed by an oblique step osteotomy at the level of the tibial tubercle, as planned in 3-D. The horizontal osteotomy is gently opened by inserting five chisels in a progressive manner posteriorly, without full engagement. The personalized wedge spacer is now introduced in the gap while giving mild valgus stress (Fig. 24.6). The two grooves on the printed wedge are checked for matching the medial cortices. The bone graft preparations are started, while the customized spacer remains in the osteotomy gap, keeping the tibia in the intended corrected position. The printed negative cast is used as a box in which the bone allograft (half femoral head) can be

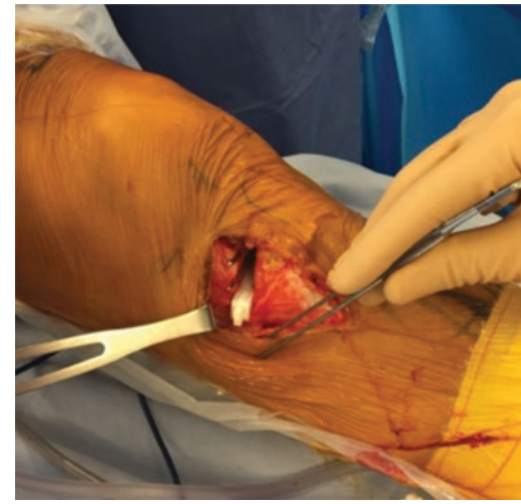

Fig. 24.6 Intraoperative introduction of the personalized wedge spacer which instantly provides the intended correction, while the identical structural bone graft is prepared

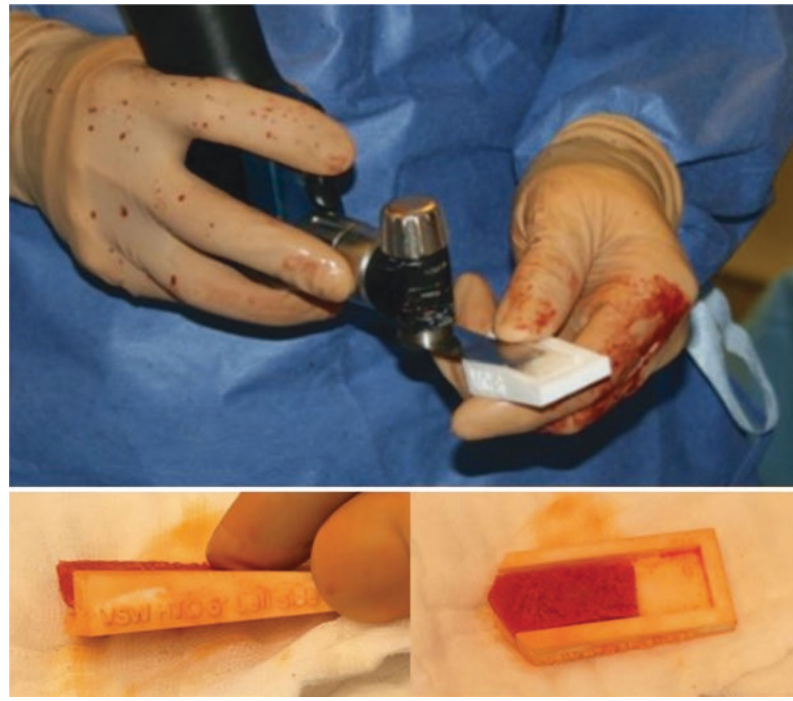

Fig. 24.7 Precise trimming of the structural bone allograft derived from half of a femur head in the dedicated cast of the patient

precisely customized. The bone allograft is trimmed triangularly by a sawblade until the size matches the original printed wedge (Fig. 24.7). When ready, the printed spacer is exchanged for the wedge-shaped structural bone graft which ultimately provides an identical alignment correction. The osteotomy is finally fixed with a TomoFix® locking plate (Depuy-Synthes GmbH, Solothurn, Switzerland).

24.5.3 Accuracy Outcome

For study purposes, ten patients that were operated according to this novel PSI technique received a full leg CT-scan and radiograph at 3 months postoperatively to assess accuracy outcomes in the coronal and sagittal plane (Table 24.2). Accuracy results showed that 90% (9/10) were within an accuracy range of [−1.5°;+1.5°] mFTA around the target, while all cases were within [−2°;+2°]. In the sagittal plane, an absolute ΔTS of 2.7° ± 1.8 was observed with an effective average slope increase of 2.1°. In comparison to previous PSI osteotomy studies (Table 24.1), our pilot study showed highly accurate and therefore similar results in the coronal plane, while assessment was performed on more reliable 3-D imaging postoperatively. However, in the sagittal plane, an unintended slight increase of the posterior slope was observed. The authors hypothesize that this might have been due to the

Table 24.2 Accuracy outcomes of the authors personal PSI technique for opening-wedge HTO

Angle	Outcome	3-D imaging (mean ± SD)	2-D imaging (mean ± SD)
mFTA (°)	Relative Δ	−0.4 ± 1.0	-0.5 ± 1.3
	Absolute Δ	0.9 ± 0.6	1.2 ± 0.7
mMPTA (°)	Relative Δ	−1.0 ± 1.4	0.3 ± 2.2
	Absolute Δ	1.3 ± 1.1	1.7 ± 1.3
TS (°)	Relative Δ	2.1 ± 2.6	0.0 ± 3.2
	Absolute Δ	2.7 ± 1.8	2.2 ± 2.2

Δ difference, *mMPTA* mechanical medial proximal tibial angle, *mFTA* mechanical femorotibial angle, *WBL* weight-bearing line, *TS* tibial slope, *SD* standard deviation

limited width of the printed wedge and structural graft (1 cm) which allowed for tibia plateau tilting in the sagittal plane. Therefore, a larger case series is currently ongoing to investigate a resized model of this PSI technique.

24.6 General Factors to Consider in 3-D Planning and PSI Osteotomy

Besides accurately obtaining the planned osteotomy correction, some practical and logistical factors need to be considered when applying 3-D planning and printing of PSI in clinical practice. Firstly, 3-D imaging in any form (CT or MRI) of the proximal tibia is minimally required to simulate the bone cut and plan the osteotomy opening in a multiplanar fashion. This might be associated with an additional cost and in case of CT-scan, with increased radiation exposure on top of a standard preoperative full-leg radiograph. The effective radiation dose of a CT-scan is largely dependent on the applied slice thickness, spacing and scanned area. Therefore, very low-dose protocols for scanning the lower limb have been established, only targeting a centred range of the hip, knee and ankle joint resulting in reliable 3-D anatomic models for planning realignment and arthroplasty surgery [20]. In this way, the effective radiation dose can be reduced to the equivalent of one full-leg standing radiograph. Altogether, the slight increase in radiation dose for 3-D planning purposes should be put in perspective to the reduced need for fluoroscopy intraoperatively when applying PSI [16, 26, 28, 36].

Primary goals of PSI are to facilitate technically demanding osteotomy surgeries, leading to reduced operating times while minimizing human correction errors [17, 36]. Perez-Mananes recorded the tourniquet time in HTO cases with and without PSI which was on average 61 and 92 minutes, respectively [26]. Similar for DFO operations, significantly reduced surgery times were observed in favour of the PSI technique [36]. In addition, the saved OR time was financially translated and yielded €522/procedure, which ultimately appeared to cover the cost of a new 3-D printer. Nevertheless, preoperative 3-D planning and printing is obviously more time-consuming relative to conventional methods and often requires the collaboration with a biomedical engineer. So, in short, the time and associated cost saved during PSI surgery can be directly reinvested in the preoperative planning and production phase of the next osteotomy patient, resulting in a sustainable and economically healthy feedback system. This is in contrast to the use of computer navigation, which is, despite delivering highly accurate corrections in lower limb realignment, prolonging the operation time, technically more demanding and very expensive on top [18, 19].

A legitimate concern, however, is the effect of PSI mal-positioning as this might potentially increase the risk of tibia plateau fractures, intra-articular screw positioning, inaccurate translation of the planning and poor clinical outcomes [46]. To assess the potential consequences, Jud et al. simulated guide mal-positioning (cutting slot with predrilled screw holes for matching plate fixation) by stepwise translation (5 mm) and rotation (2.5°) on the proximal tibia in 3-D medical software [46]. Although a proximal 5 mm translation of the guide resulted in surgical failure, the authors concluded that PSI mal-positioning was safe within the possible ‘degrees of freedom’ and had low impact on coronal accuracy. Tibial slope changes, however, were not assessed.

Finally, the experience of the surgeon should be taken into account when the accuracy and potential advantages of PSI and conventional HTO studies are investigated. The authors hypothesize that the implementation of PSI might be most beneficial in case of young or unexperienced orthopaedic surgeons performing standard knee osteotomies, since a short learning curve can be expected with most PSI guides. However, for the experienced senior surgeon, satisfying accuracy levels can potentially be obtained with conventional HTO approaches, but PSI might still be valuable in more complex surgeries such as large or rotational corrections, multiplanar deformities and double-level osteotomies.

In future perspectives, technological development might further reduce the radiation exposure and advance required imaging such as EOS weight-bearing full-leg CT-scan and cone-beam. Further, the automation of the segmentation/planning process should be stimulated and the cost of 3-D software and printers decreased to enhance the onsite accessibility of medical 3-D technology. Additionally, advanced technology with biomechanical finite element analysis will evolve, attempting to customize the fixation hardware and improve implant size and fit to the 'post-distraction' medial cortex [47, 48]. This approach might potentially result in less postoperative skin irritation and subsequently lowering the reoperation rate for hardware removal after knee osteotomies.

24.7 Conclusion

Three-dimensional osteotomy planning and PSI printing have successfully found their way into the field of knee osteotomy surgery. A handful of PSI techniques have been developed and clinically tested over the past decade, showing overall highly accurate outcomes in the coronal plane, while the tibial slope can be well-controlled. Despite these promising preliminary results, the biplanar accuracy and long-term clinical advantage over conventional HTO surgery remains to be determined in large comparative, and preferably randomized, trials. In the meantime, technological development might further (1) reduce the radiation exposure and advance required imaging, (2) stimulate the automation of the segmentation processes and (3) decrease the cost of 3-D software and printers to make medical 3-D technology accessible for the majority of hospitals. In addition, radiation exposure, costs for equipment, time-intensive preoperative planning and experience of the surgeon are factors that need to be outbalanced with the relative benefits associated with surgical accuracy. Nevertheless, in complex osteotomy cases, the authors advocate the use 3-D planning and PSI. It can guide the surgeon through the operation, leading to satisfying accuracy outcomes, as this remains one of the most important factors in the durability of joint-preserving osteotomies around the knee.

References

1. Brinkman JM, Lobenhoffer P, Agneskirchner JD, Staubli AE, Wymenga AB, Van Heerwaarden RJ. Osteotomies around the knee: patient selection, stability of fixation and bone healing in high tibial osteotomies. J Bone Jt Surg - Ser B. 2008;90(12):1548–57.
2. Liu X, Chen Z, Gao Y, Ztthang J, Jin Z. High Tibial Osteotomy: Review of Techniques and Biomechanics. J Healthc Eng. 2019;2019:8363128.
3. Bellemans J, Colyn W, Vandenneucker H, Victor J. The chitranjan ranawat award: is neutral mechanical alignment Normal for all patients? The concept of constitutional Varus. Clin Orthop Relat Res. 2012;470(1):45–53.
4. Sharma L, Song J, Felson DT, Cahue S, Shamiyeh E, Dunlop DD. The role of knee alignment in disease progression and functional decline in knee osteoarthritis. J Am Med Assoc. 2001;286(2):188–95.
5. Brouwer GM, Van Tol AW, Bergink AP, Belo JN, Bernsen RMD, Reijman M, et al. Association between valgus and varus alignment and the development and progression of radiographic osteoarthritis of the knee. Arthritis Rheum. 2007;56(4):1204–11.
6. Duivenvoorden T, Brouwer RW, Baan A, Bos PK, Reijman M, Bierma-Zeinstra SMA, et al. Comparison of closing-wedge and opening-wedge high tibial osteotomy for medial compartment osteoarthritis of the knee: a randomized controlled trial with a six-year follow-up. J Bone Joint Surg Am. 2014;96:1425–32.
7. Brouwer RW, Bierma-Zeinstra SM. A, van Raaij TM, Verhaar J a N. osteotomy for medial compartment arthritis of the knee using a closing wedge or an opening wedge controlled by a Puddu plate. A one-year randomised, controlled study. J Bone Joint Surg Br. 2006;88(11):1454–9.
8. Sabzevari S, Ebrahimpour A, Khalilipour Roudi M, Kachooei AR. High Tibial osteotomy: a systematic review and current concept. Arch Bone Jt Surg [Internet]. 2016;204(43):204–12. Available from: http://abjs.mums.ac.ir
9. Hantes ME, Natsaridis P, Koutalos AA, Ono Y, Doxariotis N, Malizos KN. Satisfactory functional and radiological outcomes can be expected in young patients under 45 years old after open wedge high tibial osteotomy in a long-term follow-up. Knee Surg Sport Traumatol Arthrosc [Internet]. 2018;26(11):3199–205. https://doi.org/10.1007/s00167-017-4816-z.
10. Schallberger A, Jacobi M, Wahl P, Maestretti G, Jakob RP. High tibial valgus osteotomy in unicompartmental medial osteoarthritis of the knee: a retrospective follow-up study over 13-21 years. Knee Surg Sports Traumatol Arthrosc. 2011 Jan;19(1):122–7.

11. Takeuchi R, Ishikawa H, Kumagai K, Yamaguchi Y, Chiba N, Akamatsu Y, et al. Fractures around the lateral cortical hinge after a medial opening-wedge high tibial osteotomy: a new classification of lateral hinge fracture. Arthrosc - J Arthrosc Relat Surg. 2012;28(1):85–94.
12. Woodacre T, Ricketts M, Evans JT, Pavlou G, Schranz P, Hockings M, et al. Complications associated with opening wedge high tibial osteotomy - a review of the literature and of 15 years of experience. Knee [Internet]. 2016;23(2):276–82. https://doi.org/10.1016/j.knee.2015.09.018.
13. Nha KW, Kim HJ, Ahn HS, Lee DH. Change in posterior Tibial slope after open-wedge and closed-wedge high Tibial osteotomy. Am J Sports Med. 2016;44(11):3006–13.
14. Fucentese SF, Meier P, Jud L, Köchli GL, Aichmair A, Vlachopoulos L, et al. Accuracy of 3D-planned patient specific instrumentation in high tibial open wedge valgisation osteotomy. J Exp Orthop. 2020;7(1):1–7.
15. Van den Bempt M, Van Genechten W, Claes T, Claes S. How accurately does high tibial osteotomy correct the mechanical axis of an arthritic varus knee? A systematic review. Knee [Internet]. 2016;23(6):925–35. https://doi.org/10.1016/j.knee.2016.10.001.
16. Jones GG, Jaere M, Clarke S, Cobb J. 3D printing and high tibial osteotomy. EFORT Open Rev [Internet]. 2018;3(5):254–9. Available from: http://online.boneandjoint.org.uk/doi/10.1302/2058-5241.3.170075
17. Sys G, Eykens H, Lenaerts G, Shumelinsky F, Robbrecht C, Poffyn B. Accuracy assessment of surgical planning and three-dimensional-printed patient-specific guides for orthopaedic osteotomies. Proc Inst Mech Eng Part H J Eng Med. 2017;231(6):499–508.
18. Saragaglia D, Roberts J. Navigated osteotomies around the knee in 170 patients with osteoarthritis secondary to genu varum. Orthopedics. 2005;28(10 Suppl):s1269–74.
19. Iorio R, Pagnottelli M, Vadalà A, Giannetti S, Di Sette P, Papandrea P, et al. Open-wedge high tibial osteotomy: comparison between manual and computer-assisted techniques. Knee Surg Sport Traumatol Arthrosc. 2013;21(1):113–9.
20. Henckel J, Richards R, Lozhkin K, Harris S, Baena FMR, Barrett ARW, et al. Very low-dose computed tomography for planning and outcome measurement in knee replacement: the imperial knee protocol. J Bone Jt Surg - Br Vol [Internet]. 2006;88-B(11):1513–8. Available from: http://www.bjj.boneandjoint.org.uk/cgi/doi/10.1302/0301-620X.88B11.17986
21. Sarment DP, Al-Shammari K, Kazor CE. Stereolithographic surgical templates for placement of dental implants in complex cases. Int J Periodontics Restorative Dent [Internet]. 2003;23(3):287–95. Available from: http://www.ncbi.nlm.nih.gov/pubmed/12854779
22. Lu S, Zhang YZ, Wang Z, Shi JH, Chen YB, Xu XM, et al. Accuracy and efficacy of thoracic pedicle screws in scoliosis with patient-specific drill template. Med Biol Eng Comput [Internet]. 2012;50(7):751–8. Available from: http://www.ncbi.nlm.nih.gov/pubmed/22467276
23. Byrne A-M, Impelmans B, Bertrand V, Van Haver A, Verstreken F. Corrective osteotomy for Malunited Diaphyseal forearm fractures using preoperative 3-dimensional planning and patient-specific surgical guides and implants. J Hand Surg Am [Internet]. 2017;42(10):836.e1–836.e12. Available from: http://www.ncbi.nlm.nih.gov/pubmed/28709790
24. Victor J, Premanathan A. Virtual 3D planning and patient specific surgical guides for osteotomies around the knee: a feasibility and proof-of-concept study. Bone Joint J. 2013;95 B(11 Suppl A):153–8.
25. Munier M, Donnez M, Ollivier M, Flecher X, Chabrand P, Argenson JN, et al. Can three-dimensional patient-specific cutting guides be used to achieve optimal correction for high tibial osteotomy? Pilot study. Orthop Traumatol Surg Res [Internet]. 2017;103(2):245–50. https://doi.org/10.1016/j.otsr.2016.11.020.
26. Pérez-Mañanes R, Burró JA, Manaute JR, Rodriguez FC, Martín JV. 3D surgical printing cutting guides for open-wedge high Tibial osteotomy: do it yourself. J Knee Surg. 2016;29(8):690–5.
27. Kim H-J, Park J, Shin J-Y, Park I-H, Park K-H, Kyung H-S. More accurate correction can be obtained using a three-dimensional printed model in open-wedge high tibial osteotomy. Knee Surg Sport Traumatol Arthrosc [Internet]. 2018;26:3452–8. Available from: http://link.springer.com/10.1007/s00167-018-4927-1.
28. Yang JCS, Chen CF, Luo CA, Chang MC, Lee OK, Huang Y, et al. Clinical experience using a 3D-printed patient-specific instrument for medial opening wedge high Tibial osteotomy. Biomed Res Int. 2018;2018:1–9.
29. Schröter S, Ihle C, Mueller J, Lobenhoffer P, Stöckle U, van Heerwaarden R. Digital planning of high tibial osteotomy. Interrater reliability by using two different software. Knee Surgery, Sport Traumatol Arthrosc. 2013;21(1):189–96.
30. Swanson KE, Stocks GW, Warren PD, Hazel MR, Janssen HF. Does axial limb rotation affect the alignment measurements in deformed limbs? Clin Orthop Relat Res. 2000;371:246–52.
31. Koshino T, Takeyama M, Jiang LS, Yoshida T, Saito T. Underestimation of varus angulation in knees with flexion deformity. Knee. 2002;9(4):275–9.
32. Kawakami H, Sugano N, Yonenobu K, Yoshikawa H, Ochi T, Hattori A, et al. Effects of rotation on measurement of lower limb alignment for knee osteotomy. J Orthop Res. 2004;22(6):1248–53.
33. Specogna AV, Birmingham TB, Hunt MA, Jones IC, Jenkyn TR, Fowler PJ, et al. Radiographic measures of knee alignment in patients with varus gonarthrosis: effect of weightbearing status and associations with dynamic joint load. Am J Sports Med. 2007;35(1):65–70.
34. Ogawa H, Matsumoto K, Ogawa T, Takeuchi K, Akiyama H. Preoperative varus laxity correlates with overcorrection in medial opening wedge

high tibial osteotomy. Arch Orthop Trauma Surg. 2016;136(10):1337–42.
35. Lee YS. Eu., Kim MG y., Byun HW o., Kim SB u., Kim JG o. reliability of the imaging software in the preoperative planning of the open-wedge high tibial osteotomy. Knee Surg Sports Traumatol Arthrosc. 2015;23(3):846–51.
36. Arnal-Burró J, Pérez-Mañanes R, Gallo-del-Valle E, Igualada-Blazquez C, Cuervas-Mons M, Vaquero-Martín J. Three dimensional-printed patient-specific cutting guides for femoral varization osteotomy: do it yourself. Knee. 2017;24(6):1359–68.
37. Chaouche S, Jacquet C, Fabre-Aubrespy M, Sharma A, Argenson JN, Parratte S, et al. Patient-specific cutting guides for open-wedge high tibial osteotomy: safety and accuracy analysis of a hundred patients continuous cohort. Int Orthop. 2019;43(12):2757–65.
38. DePuy Orthopaedics. Radiation exposure considerations with the use of TruMatch personalized solutions. 2010.
39. Kubota M, Ohno R, Sato T, Yamaguchi J, Kaneko H, Kaneko K. The medial proximal tibial angle accurately corrects the limb alignment in open-wedge high tibial osteotomy. Knee Surg Sport Traumatol Arthrosc [Internet]. 2018;27:1–7. https://doi.org/10.1007/s00167-018-5216-8.
40. Nakayama H, Schröter S, Yamamoto C, Iseki T, Kanto R, Kurosaka K, et al. Large correction in opening wedge high tibial osteotomy with resultant joint-line obliquity induces excessive shear stress on the articular cartilage. Knee Surg Sport Traumatol Arthrosc. 2018;26(6):1873–8.
41. Chernchujit B, Tharakulphan S, Prasetia R, Chantarapanich N, Jirawison C, Sitthiseripratip K. Preoperative planning of medial opening wedge high tibial osteotomy using 3D computer-aided design weight-bearing simulated guidance: technique and preliminary result. J Orthop Surg. 2019;27(1):1–8.
42. Victor J, Van Doninck D, Labey L, Innocenti B, Parizel PM, Bellemans J. How precise can bony landmarks be determined on a CT scan of the knee? Knee [Internet]. 2009;16(5):358–65. https://doi.org/10.1016/j.knee.2009.01.001.
43. Auricchio F. Instructional lecture : general Orthopaedics 3D printing : clinical applications in orthopaedics and traumatology. EFORT Open Rev. 2016;1(May):121–7.
44. Kwun JD, Kim HJ, Park J, Park IH, Kyung HS. Open wedge high tibial osteotomy using three-dimensional printed models: experimental analysis using porcine bone. Knee [Internet]. 2017;24(1):16–22. https://doi.org/10.1016/j.knee.2016.09.026.
45. Donnez M, Ollivier M, Munier M, Berton P, Podgorski JP, Chabrand P, et al. Are three-dimensional patient-specific cutting guides for open wedge high tibial osteotomy accurate? An in vitro study. J Orthop Surg Res. 2018;13(1):1–8.
46. Jud L, Fürnstahl P, Vlachopoulos L, Götschi T, Leoty LC, Fucentese SF. Malpositioning of patient-specific instruments within the possible degrees of freedom in high-tibial osteotomy has no considerable influence on mechanical leg axis correction. Knee Surgery, Sport Traumatol Arthrosc [Internet]. 2019;28(5):1356–64. https://doi.org/10.1007/s00167-019-05432-3.
47. Koh YG, Lee JA, Lee HY, Chun HJ, Kim HJ, Kang KT. Design optimization of high tibial osteotomy plates using finite element analysis for improved biomechanical effect. J Orthop Surg Res. 2019;14(1):1–10.
48. Yoo OS, Lee YS, Lee MC, Park JH, Kim JW, Sun DH. Morphologic analysis of the proximal tibia after open wedge high tibial osteotomy for proper plate fitting. BMC Musculoskelet Disord [Internet]. 2016;17(1):1–9. https://doi.org/10.1186/s12891-016-1277-3.